Bull Mater Sci (2020) 43:226
https://doi.org/10.1007/s12034-020-02186-4

tert-Butylamine borane as a reductant in electroless nickel plating for improved etch resistance in the electrolyte

SOLLEE KIM and SUKEUN YOON*
Division of Advanced Materials Engineering, Institute for Rare Metals, Kongju National University, Chungnam 31080, Republic of Korea
*Author for correspondence (skyoon@kongju.ac.kr)

MS received 22 November 2019; accepted 13 February 2020

Abstract. An Ni–B coating was developed on a copper substrate by the direct electroless technique and from a plating bath containing *tert*-butylamine borane (TBAB). The influence of the electroless plating conditions, using TBAB as a reducing agent on the composition, surface morphology, high-temperature stability and etch resistance in the electrolyte of the coatings, was investigated. The resulting electroless Ni–B plating surfaces were examined and characterized by scanning electron microscopy and X-ray fluorescence spectroscopy for morphology and chemical composition, respectively. Electrochemical characterization by potentiodynamic polarization confirmed that a 0.1 M nickel concentration bath for the Ni–B plating was optimized by a TBAB concentration of 0.03 M, temperature of 60°C and pH of 8. Under the optimal bath conditions, the Ni–B electroless plating layer exhibited superior etch resistance in the electrolyte as well as improved stability at high temperature than the Ni–B electroless plating layer prepared using dimethylamine borane. Hence, owing to the remarkable properties of the Ni–B electroless plating layer, this fabrication technique that employs TBAB can be extended to fabricate other Ni–B electroless plating layers.

Keywords. Electroless plating; Ni–B alloy; *tert*-butylamine borane; deposition rate; electrolyte resistance.

1. Introduction

Since the inception of Ni electroless plating by Brenner and Riddell in 1946, this technique, which offers good adhesion and uniform thickness, has been widely studied because it can be employed not only for metal materials but also for non-conductive surfaces, such as plastics and ceramics [1,2]. Ni electroless plating techniques are generally classified as Ni–P, Ni–B and pure Ni or Ni-based alloys depending on the reducing agents (i.e., sodium hypophosphite (NaH_2PO_2), sodium borohydride ($NaBH_4$), dimethylamine borane (DMAB, C_2H_7BN) and hydrazine (NH_2NH_2) in the plating bath [3–7]. In particular, among them, Ni–P electroless reduction by sodium hypophosphite has enjoyed commercial success owing to its low cost, workability and excellent physical properties of the coating [8]. However, the usage of the Ni–B electroless plating method has been relatively limited owing to the higher cost incurred, as well as greater sensitivity of this method to impurities than Ni–P electroless plating method using hypophosphite. This, despite the distinct advantages of an Ni–B electroless coating compared to an Ni–P electroless coating, in terms of its high hardness and low friction coefficient, results in better etch resistance [9,10].

Ni–B coatings are typically prepared using different sulphamates and the Watts bath with boron-containing reducing agents, such as sodium borohydride, DMAB, trimethylamine borane (TMAB) or sodium decahydrodecarborate ($Na_2B_{10}H_{10}$). It has been observed that the co-deposited boron content maintains the Ni reduction rate constant by controlling effective parameters, such as the current density, temperature, agitation and pH during electrodeposition; this ability of the co-deposited boron is strongly influenced by the type of boron source [11]. Sodium borohydride can provide up to eight electrons for the reduction of some metals, resulting in high reduction efficiency as well as cost-effectiveness of operation. However, the borohydride ion is easily hydrolysed in acid or neutral solutions to spontaneously yield nickel boride in the presence of nickel ions in the plating bath. As a result, the composition and structure of the coating layer can be easily changed [12]. In contrast, DMAB, when used as a reducing agent, can improve the stability of the plating bath over a wide pH range, allow operation at a relatively low temperature and maintain the bath composition constant, compared to sodium borohydride. Particularly, electroless plating baths using DMAB are typically used for the electroless plating of components for electronic applications owing to their ability to operate at a relatively lower temperature [6,13].

Nickel plating is also an important technique in the field of rechargeable battery components. The lead tab (electrode

Published online: 20 August 2020

terminal) electrically connects the inside of the battery and the outside of the battery and is divided into an Al terminal for a positive electrode and Ni-plated Cu for a negative electrode. Recently, the demand for high-performance rechargeable batteries has increased; concurrently, lead tabs now require properties, such as increased conductivity, corrosion resistance and hydrofluoric (HF) acid resistance, to increase the high-power density and durability [14]. Nickel plating for lead tabs typically involves Ni–P electrolytic or electroless plating. However, Ni–B plating has recently been necessitated because it is difficult to manage the plating bath in Ni–P plating. In addition, Ni–B plating has not been attempted to scientifically investigate the corrosion resistance and HF resistance for the use of this plating layer in lead tabs of lithium-ion batteries.

Herein, we aimed to elucidate the effect of *tert*-butylamine borane (TBAB) as a boron reduction source on the Ni–B surface properties and electroless conditions, and by comparison with Ni–B surfaces using DMAB, determine whether it can improve the electrolyte resistance in lead tab materials of rechargeable batteries.

2. Experimental

2.1 *Sample preparation*

The procedure of Ni–B alloy electroless plating on a Cu substrate is illustrated in figure 1. Ni–B alloy deposition was conducted on a commercially available Cu substrate ($10 \times 10 \times 1$ mm^3). Prior to electroplating (for nickel strike), the specimen was pre-treated with 7% H_2SO_4 solution at 25°C for 12 s to sensitize and activate the Cu surface and was then rinsed with deionized water. The specimen was then subjected to Wood's nickel strike process to prepare the substrate for electroless deposition. The chemical composition of Wood's nickel strike is as follows: 45 g l^{-1} $NiCl_2$, 240 g l^{-1} $NiSO_4{\cdot}6(H_2O)$ and 30 g l^{-1} H_3BO_3; the process conditions were a pH of 4.5, temperature of 50°C and a constant voltage of 6 V applied for 12 s. The Ni–B alloy electroless plating solution with its pH adjusted to 6 in this study was composed of a mixture of 0.1 M nickel sulphate hexahydrate ($NiSO_4{\cdot}6(H_2O)$, >98%, Alfa Aesar) as the nickel source, 0.1 M citric acid ($C_6H_8O_7$, >99%, Aldrich) as the complexing agent, 2 ppm lead nitrate ($Pb(NO_3)_2$, >99%, Aldrich) as the stabilizing agent and TBAB ($(CH_3)_3CNH_2{\cdot}BH_3$, >97%, Alfa Aesar) as the reducing agent. Ni–B alloy electroless plating was then carried out using this plating bath with varying reducing agent concentrations (0.01–0.1 M) and pH values (6–8) at 60°C. And then, five specimens were prepared and analysed for each sample of the Ni–B alloy electroless plating pieces. For comparison of the Ni–B alloy electroless plating, Ni–B alloy electroless plating samples were prepared using DMAB ($(CH_3)_2NH{\cdot}BH_3$, >97%, Alfa Aesar) as the reducing agent under the same conditions of the electroless plating solution using TBAB.

2.2 *Sample characterization*

The surface morphology and microstructure of the electroless Ni–B plating samples were examined by scanning electron microscopy (SEM, Tescan Mira LM). Five Ni–B plating specimens were prepared, and the composition and thickness of each was determined by X-ray fluorescence (Rigaku ZSX Primus) analysis.

A conventional three-electrode system was used for the electrochemical measurements, with a saturated calomel electrode (SCE) as the reference electrode, graphite electrode as the counter electrode and the nickel-strike-treated sample as the working electrode. Potentiodynamic polarization of the Ni–B plating sample with a working surface area of 1 cm^2 was conducted with a ZIVE SP2

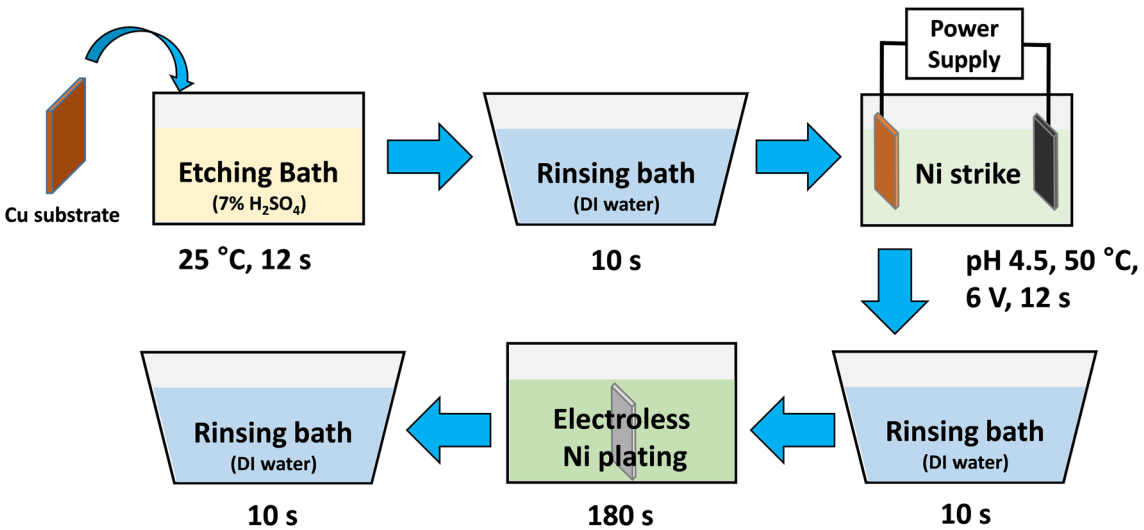

Figure 1. Technical flow chart of Ni–B electroless plating.

potentiostat/galvanostat in various Ni–B plating bath conditions at a potential scanning rate of 2 mV s^{-1}.

The etch resistance in the electrolyte was determined by immersing the Ni–B plating sample in an electrolyte containing 1 M $LiPF_6$ in a mixture of ethylene carbonate and diethyl carbonate (1:1 v/v) at 80°C for 24 h. The high-temperature stability of the Ni–B plating samples was determined after sintering at 450°C for 24 h.

3. Results and discussion

Electroless plating, which is an autocatalytic electrochemical reaction, occurs at a potential where the partial cathodic polarization curve of the nickel ion and the partial anodic polarization curve of TBAB overlap by the mixed potential theory. Figure 2a shows the variation in the deposition potential according to the concentration of TBAB as a reducing agent at 60°C, pH 6 and in a 0.1 M nickel bath. The deposition potential was shifted in the negative direction at 0.03 M TBAB with increasing current density for anodic polarization. Subsequently, even when the TBAB concentration is increased, the deposition potential did not increase along the direction of the negative potential, and the current density decreases. The deposition rates according to the TBAB concentration were calculated by the gravimetric method and are compared in figure 2b. As the TBAB concentration increased until 0.03 M in the 0.1 M nickel ion bath, the oxidation/reduction reaction was equilibrated and showed the maximum electrodeposition rate. Thereafter, the deposition rate did not exhibit a concentration effect by the reducing agent because the nickel ion concentration in the nickel bath that could participate in the reduction reaction was lower than the TBAB concentration, making it difficult for equilibrium to occur in the redox reaction.

Figure 3a shows the partial polarization curves for the anodic oxidation and cathodic reduction of the nickel ion in the 0.1 M nickel plating solution using a reducing agent of 0.03 M TBAB under various pH conditions. The temperature of the Ni nickel bath was fixed at 60°C. With the pH increasing as 6, 7 and 8, the mixed potential and current were -0.370 V/6.03×10^{-5} A, -0.405 V/6.61×10^{-5} A and -0.502 V/8.91×10^{-5} A, respectively. As the pH of the plating solution increased, the mixed potential decreased and the current increased. This is because the partial cathodic and anodic curves shifted towards the more reversible reaction due to the increased alkalinity at a constant nickel concentration. In addition, the decrease in the mixed potential with increasing pH was because the

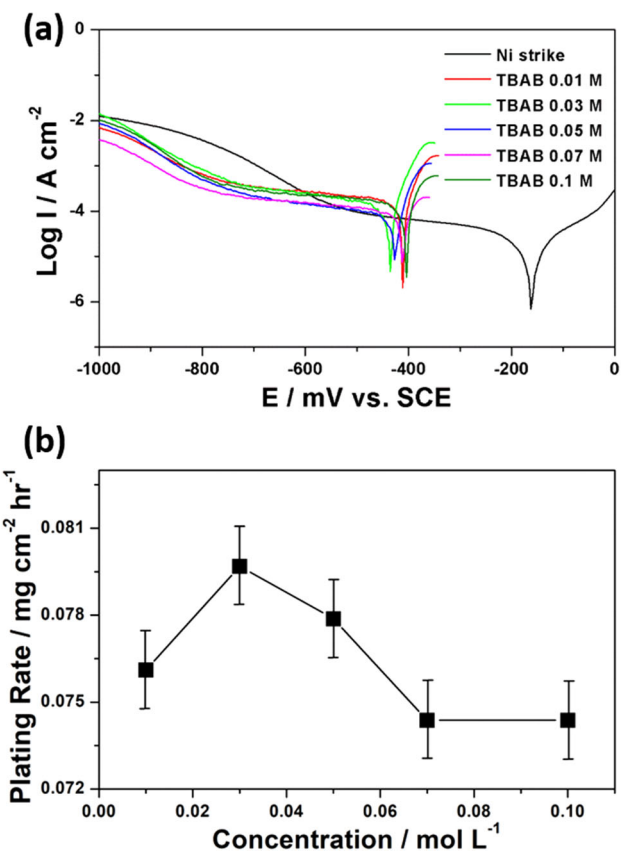

Figure 2. Effect of varying TBAB concentrations on (**a**) polarization curves and (**b**) electroplating rates.

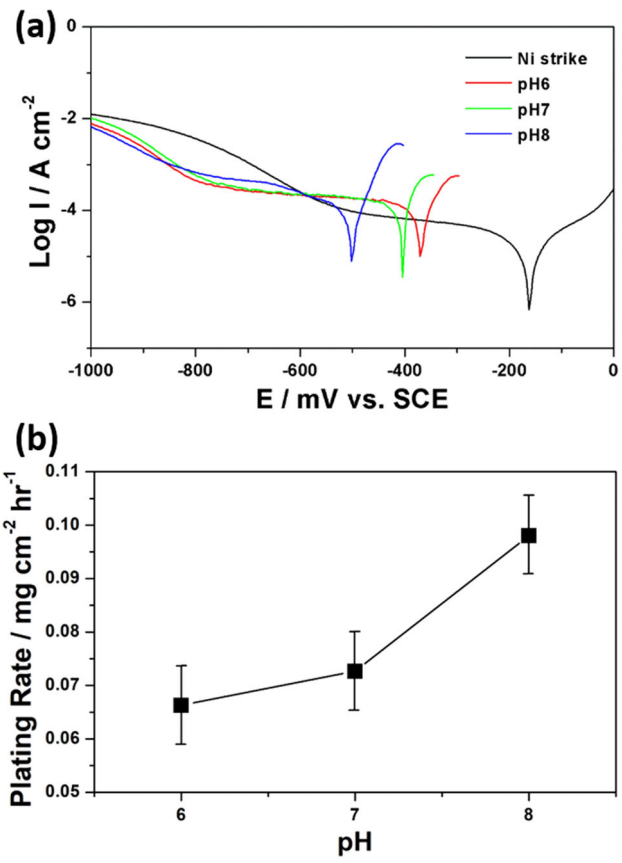

Figure 3. Effect of varying pH values on (**a**) polarization curves and (**b**) electroplating rates.

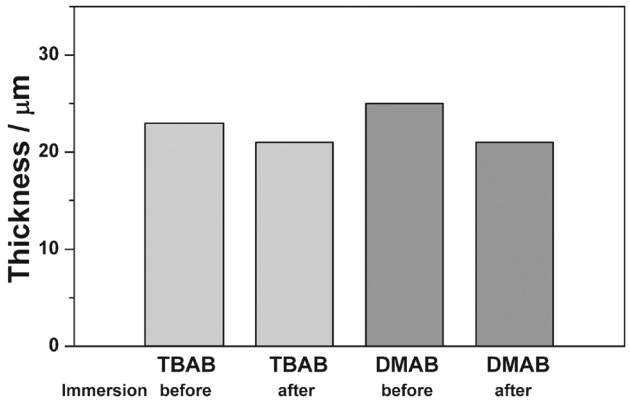

Figure 4. Comparison of thickness of Ni–B plating samples using TBAB and DMAB before and after immersion in the electrolyte.

partial anodic reaction was more influenced by the pH than by the partial cathodic reaction. This suggests that TBAB reacts as follows:

$$BH_n(OH)^-_{4-n} \rightarrow BH_{n-1}(OH)^-_{4-n} + H$$
$$BH_{n-1}(OH)^-_{4-n} + OH^- \rightarrow BH_{n-1}(OH)^-_{5-n} + e^-$$

where n is a number between 1 and 4. The hydrogen atoms could be recombined or oxidized to form water. Increasing the pH of the nickel plating solution promotes the oxidation of TBAB [15]. The plating rate calculated by the gravimetric method in figure 3b is also confirmed to increase with increasing pH, as indicated by the above polarization curves.

Following electrochemical analysis, it was confirmed that the Ni–B plating bath using TBAB as a reducing agent at 0.1 M nickel concentration was optimal when the TBAB concentration was 0.03 M and pH was 8. Therefore, we used this optimum nickel plating solution to perform Ni–B electroless plating at 60°C for 90 s. Then Ni and B composition in Ni–B electroless plating sample synthesized by optimum nickel plating solution using TBAB were 97 and 3 wt%, respectively. On the contrary, the case of DMAB was 98 and 2 wt% for Ni and B, respectively.

To determine the etch resistance of the nickel plating layer in the electrolyte, the Ni–B electroless plating sample was carried in the organic electrolytic for Li-ion batteries and then held at 80°C for 24 h. Figure 4 shows the changes in the thickness of the plating layer before and after immersion in the electrolyte solution. The thickness of the Ni–B electroless plating layer decreased from 23 to 21 μm after immersion in the electrolyte. To compare the etch resistance of the Ni–B electroless plating layer in the electrolyte using TBAB, the reducing agent was changed to DMAB under the same nickel plating bath condition, and the Ni–B electroless plating layer was analysed after immersion in the electrolyte. The thickness of the Ni–B electroless plating layer using DMAB changed from 25 to 21 μm due to the reaction of a large amount of nickel in the Ni–B electroless plating layer with the electrolyte before and after immersion in the electrolyte.

Figure 5 shows optical and SEM images of the surface morphology of the Ni–B plating samples before and after immersion in the electrolyte. After Ni–B electroless plating, we obtain visual confirmation from figure 5a that the Cu surface has been reduced to the Ni–B electroless plating layer. When the etching resistance to the electrolyte is weak, peeling or partial colour change of the plating layer is generally observed. However, these samples are shown in figure 5a, even after immersion in the electrolyte at 80°C for 24 h, no significant colour change (like dark grey) was observed. This suggests that the Ni–B electroless plating layer reduced by TBAB or DMAB is etch resistant to the electrolyte. In order to confirm the etch resistance of the

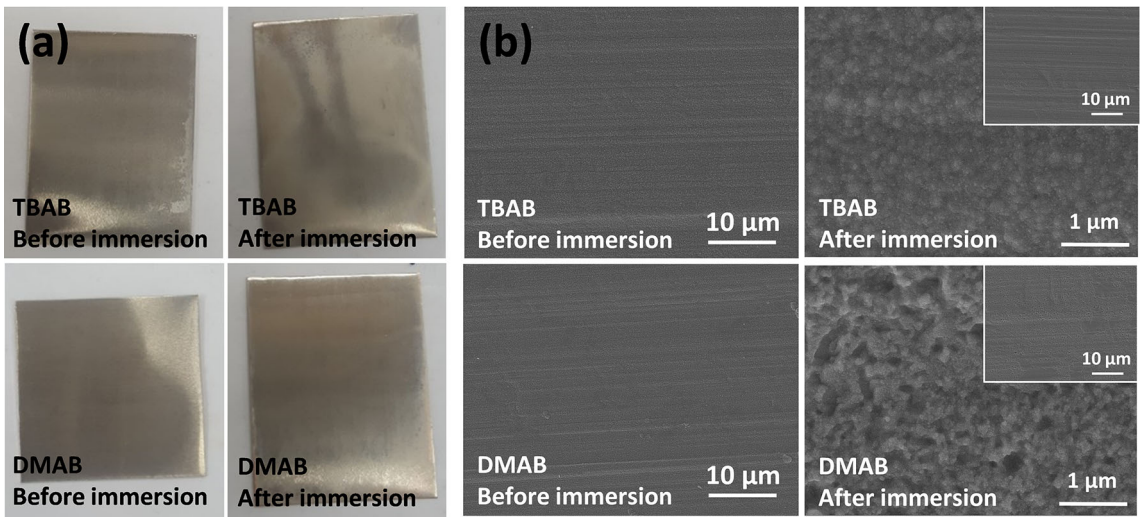

Figure 5. Comparison of (**a**) optical and (**b**) SEM images of Ni–B plating samples using TBAB and DMAB before and after immersion in the electrolyte.

Ni–B plating samples in detail, SEM surface observation was conducted, as shown in figure 5b and compared with that of the sample using DMAB as the reducing agent. Ni–B electroless plating samples using TBAB and DMAB exhibited a smooth surface. However, in the SEM images observed after immersion in the electrolyte, homogeneous hemispheres were observed for TMAB, whereas non-uniform pores were observed with DMAB due to surface peeling. This suggests that the Ni–B electroless plating layer produced by TBAB exhibits better etch resistance in electrolyte than the layer produced by DMAB. Consequentially, TBAB has distinct advantages over DMAB, which is the typical reducing agent for forming stable Ni–B electroless plating layers.

4. Conclusion

In summary, we successfully prepared Ni–B plating layers by an electroless plating method. The influence of the plating conditions, using TBAB as the reducing agent and the electrolyte resistance of the Ni–B electroless plating, was investigated. Characterization by potentiodynamic polarization confirmed that the Ni–B plating bath using TBAB as a reducing agent at 0.1 M nickel concentration was optimized at 0.03 M TBAB concentration, temperature of 60°C and a pH of 8. In addition, the Ni–B electroless plating layer exposed to optimal bath conditions for 90 s exhibited superior etch resistance when immersed in the electrolyte and was stable at high temperature. Thus, remarkable properties of the Ni–B electroless plating layer can be achieved using TBAB as a reducing agent, and this strategy can be extended to the fabrication of other Ni–B electroless plating layers.

Acknowledgement

This work was supported by the research grant of the Kongju National University in 2018 (Grant No. 2018-0299-01).

References

[1] Brenner A and Riddell G E 1946 *J. Res. Natl. Bur. Stand.* **37** 31
[2] Krishnan K H, John S, Srinivasan K N, Praveen J, Ganesan M and Kavimani P M 2006 *Metall. Mater. Trans. A* **37** 1917
[3] Shaigan N, Ashrafizadeh S N, Bafghi M S H and Rastegari S 2005 *J. Electrochem. Soc.* **152** C173
[4] Anderson S P and Kalu E E 2013 *Crystals* **3** 405
[5] Sun R, Yu G, Xie Z, Hu B, Zhang J, He X *et al* 2015 *Int. J. Electrochem. Sci.* **10** 7893
[6] Chang C R, Hou K H, Ger M D and Wang J R 2017 *Int. J. Electrochem. Sci.* **12** 2055
[7] Zhang X and Zhang J 2016 *RSC Adv.* **6** 30695
[8] Ashtiani A A, Faraji S, Iranagh S A and Faraji A H 2017 *Arabian J. Chem.* **10** S1541
[9] Anik M, Körpe E and Şen E 2008 *Surf. Coat. Technol.* **202** 1718
[10] Rha S K, Baek S D and Lee Y S 2015 *J. Nanosci. Nanotechnol.* **15** 7444
[11] Mirak M and Akbari A 2018 *Surf. Coat. Technol.* **349** 442
[12] Krishnaveni K, Sankara Narayanan T S N and Seshadri S K 2005 *Surf. Coat. Technol.* **190** 115
[13] Baskaran I, Kumar R S, Sankara Narayanan T S N and Stephen A 2006 *Surf. Coat. Technol.* **200** 6888
[14] Dai S, Chen J, Ren Y, Liu Z, Chen J, Li C *et al* 2017 *Int. J. Electrochem. Sci.* **12** 10589
[15] Liao Y, Zhang S and Dryfe R 2012 *Particuology* **10** 487